

Supplementary Materials

Improved Methanol-to-Formate Electrocatalytic Reaction by Engineering of Nickel Hydroxide and Iron Oxyhydroxide Heterostructures

Ning Jian^{1,2}, Huan Ge^{1,2}, Yi Ma^{1,2}, Yong Zhang^{1,2}, Luming Li^{1,2}, Junfeng Liu³, Jing Yu⁴, Canhuang Li⁴, and Junshan Li^{1,2,*}

¹ School of Mechanic Engineering, Chengdu University, Chengdu 610106, China

² Institute for Advanced Study, Chengdu University, Chengdu 610106, China

³ Institute for Energy Research, Jiangsu University, Jiangsu 212013, China

⁴ Catalonia Institute for Energy Research-IREC, Sant Adrià de Besòs, Barcelona 08930, Spain

* Correspondence: lijunshan@cdu.edu.cn

SEM Characterization

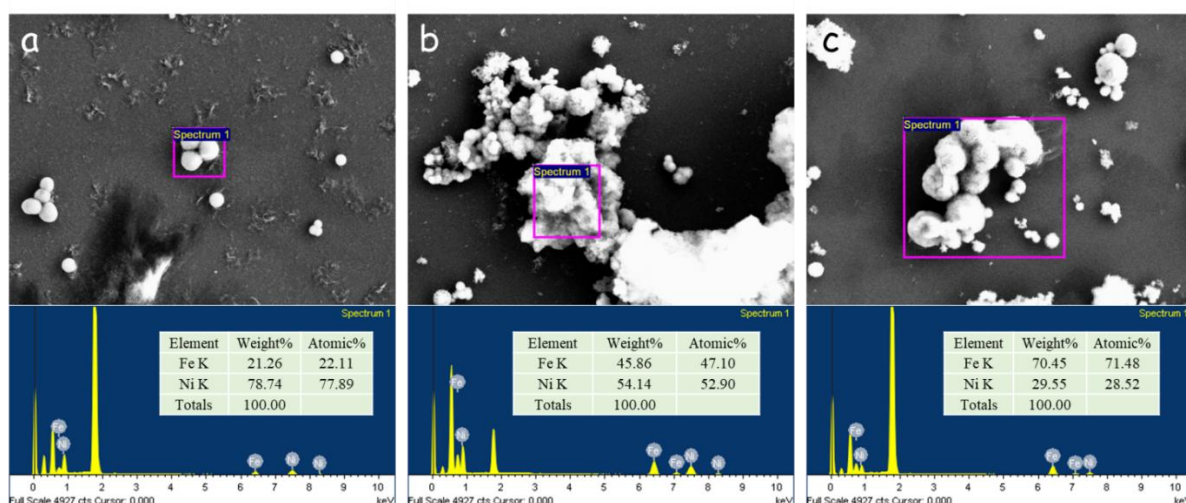


Figure S1. SEM-EDS results for the samples obtained from Ni/Fe ratio with (a) 3:1, (b) 1:1, and (c) 1:3 in the precursor.

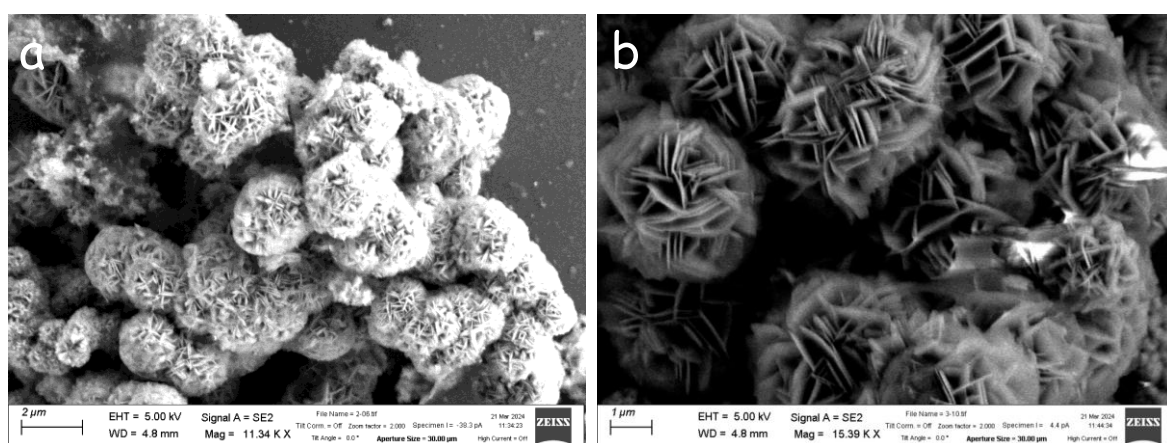


Figure S2. Representative SEM images for (a) Ni_{0.75}Fe_{0.25} and (b) Ni_{0.25}Fe_{0.75} based NFHs.



Copyright: © 2025 by the authors. This is an open access article under the terms and conditions of the Creative Commons Attribution (CC BY) license (<https://creativecommons.org/licenses/by/4.0/>).

Publisher's Note: Scilight stays neutral with regard to jurisdictional claims in published maps and institutional affiliations.

Standard IC Curve

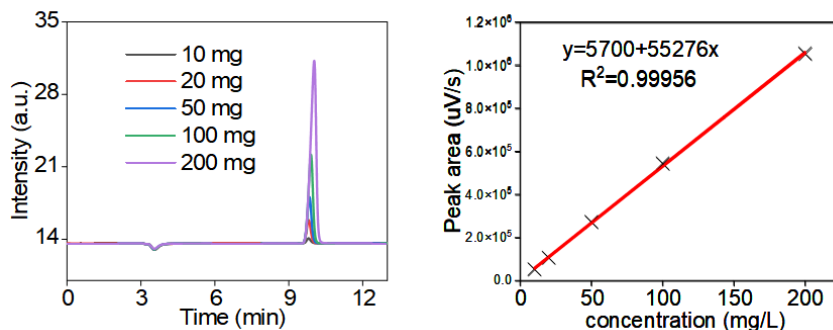


Figure S3. Standard IC profile for formate concentration and the corresponding fitting formate peak area and concentration.

Electrochemical Characterization

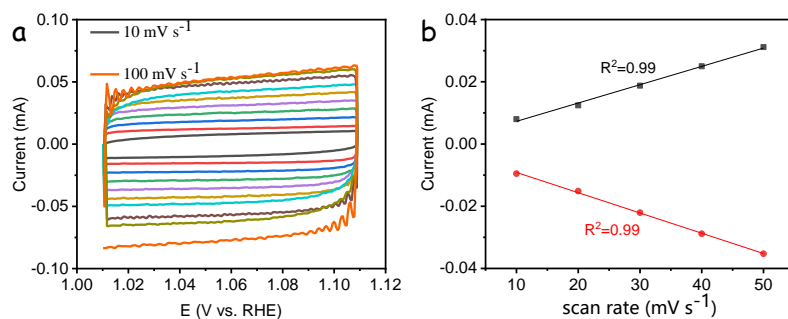


Figure S4. Determination of ECSA curves in 1 M KOH for the Ni_{0.75}Fe_{0.25}-based electrode.

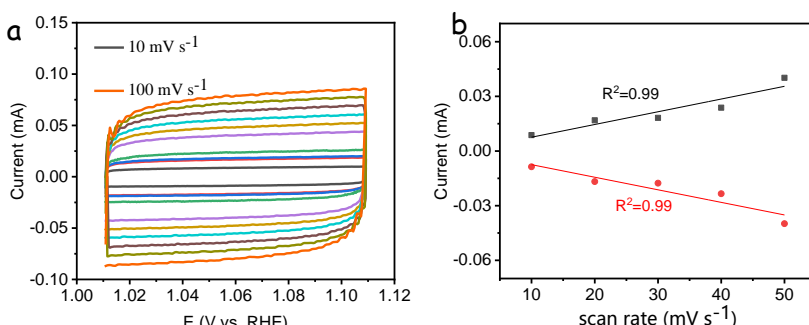


Figure S5. Determination of ECSA curves in 1 M KOH for the Ni_{0.25}Fe_{0.75}-based electrode.

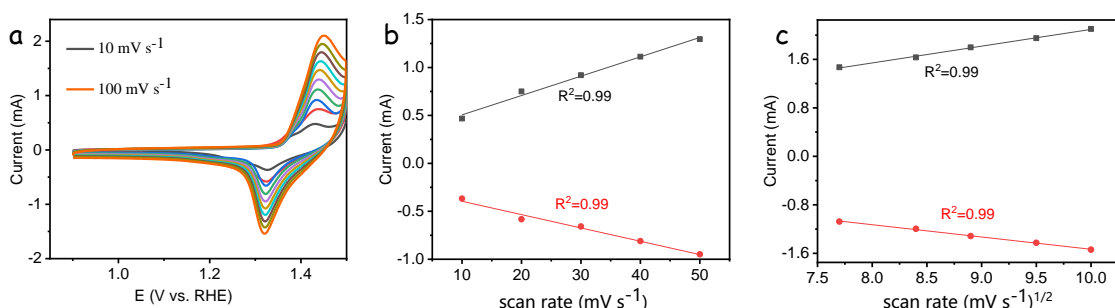


Figure S6. Intrinsic property for the Ni_{0.75}Fe_{0.25}-based electrode in 1 M KOH (a) CVs, (b) surface coverage of redox species (Γ^*), and (c) diffusion coefficient (D).

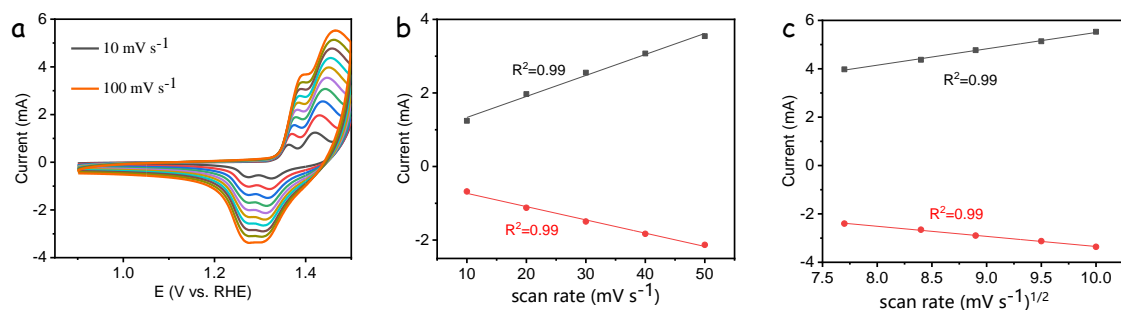


Figure S7. Intrinsic property for the Ni_{0.25}Fe_{0.75}-based electrode in 1 M KOH (a) CVs, (b) surface coverage of redox species (Γ^*), and (c) diffusion coefficient (D).

Table S1. Comparison of MOR performance between this work and previously published noble-metal-free electrocatalysts.

electrocatalyst	morphology	electrolyte	MOR performance				reference
			current density (mA cm ⁻² @V. RHE)	decay	product	FE	
Co(OH) ₂ @HOS/CP	3D nanosheet	1 M KOH + 3 M methanol	~80@1.5 V	~5% @20h	CP formate	100%	[1]
Ni–Fe Oxide	porous	1 M KOH + 1 M methanol	~15@1.6 V	~5% @ 12h	CP formate	n.a.	[2]
Ni _{0.75} Cu _{0.25} alloys	3D nanostructures	1 M NaOH + 0.5 M methanol	~45@1.6 V	~22% @0.33h	n.a.	n.a.	[3]
NiS	nanoparticles	1 M KOH + 1 M methanol	~145@1.6 V	~43% @2.78h	formate	98%	[4]
Ni _x Fe _{1-x} (OH) ₂	coreshell particle	1 M KOH + 1 M methanol	~10@1.55 V	n.a.	n.a.	n.a.	[5]
NiCo/Nickel foam	porous	1 M KOH + 2 M methanol	~82@1.5 V	~29% @12.5h	n.a.	n.a.	[6]
Ni ₃ S ₂ /CNTs	nanocrystals	1 M KOH + 1 M methanol	100@1.36 V	~1% @20h	formate	95%	[7]
Ni _{0.75} Fe _{0.25} Se ₂	nanoparticles	1 M KOH + 1 M methanol	53.3@1.5 V	27.4% @13.9h	formate	99%	[8]
Ni/MOF	nanosheet	1 M KOH + 0.5 M methanol	100@1.44 V	18.7% @20h	formate	n.a.	[9]
NiCo ₂ S ₄ /CC	nanosheet	1 M KOH + 1 M methanol	~20@1.61 V	~10% @20h	formate	100%	[10]
Formate							
NiO/NF	porous	1 M KOH + 2 M methanol	135@1.5 V	10% @2.78h	CO ₃ ²⁻	n.a.	[11]
HCHO							
Mn-NiFe LDH/NF	nanosheet	1 M KOH + 0.5 M methanol	~300@1.5 V	~15% @120h	formate	99%	[12]
Ni(OH) ₂ /FeOOH	3D flower	1 M KOH + 1 M methanol	~95@1.6 V	~45% @12h	formate	98.5%	this work

Reference

1. Xiang, K.; Wu, D.; Deng, X.; Li, M.; Chen, S.; Hao, P.; Guo, X.; Luo, J.L.; Fu, X.Z. Boosting H₂ Generation Coupled with Selective Oxidation of Methanol into Value-Added Chemical over Cobalt Hydroxide@Hydroxysulfide Nanosheets Electrocatalysts. *Adv. Funct. Mater.* **2020**, *30*, 1909610. <https://doi.org/10.1002/adfm.201909610>.
2. Mondal, B.; Karjule, N.; Singh, C.; Shimoni, R.; Volokh, M.; Hod, I.; Shalom, M. Unraveling the Mechanisms of Electrocatalytic Oxygenation and Dehydrogenation of Organic Molecules to Value-Added Chemicals Over a Ni–Fe Oxide Catalyst. *Adv. Energy Mater.* **2021**, *11*, 2101858. <https://doi.org/10.1002/AENM.202101858>.
3. Cui, X.; Xiao, P.; Wang, J.; Zhou, M.; Guo, W.; Yang, Y.; He, Y.; Wang, Z.; Yang, Y.; Zhang, Y.; et al. Highly Branched Metal Alloy Networks with Superior Activities for the Methanol Oxidation Reaction. *Angew. Chem.-Int. Ed.* **2017**, *56*, 4488–4493. <https://doi.org/10.1002/anie.201701149>.
4. Li, J.; Tian, X.; Wang, X.; Zhang, T.; Spadaro, M.C.; Arbiol, J.; Li, L.; Zuo, Y.; Cabot, A. Electrochemical Conversion of Alcohols into Acidic Commodities on Nickel Sulfide Nanoparticles. *Inorg. Chem.* **2022**, *61*, 13433–13441. <https://doi.org/10.1021/acs.inorgchem.2c01695>.
5. Candelaria, S.L.; Bedford, N.M.; Woehl, T.J.; Rentz, N.S.; Showalter, A.R.; Pylypenko, S.; Bunker, B.A.; Lee, S.; Reinhart, B.; Ren, Y.; et al. Multi-Component Fe-Ni Hydroxide Nanocatalyst for Oxygen Evolution and Methanol Oxidation Reactions under Alkaline Conditions. *ACS Catal.* **2017**, *7*, 365–379. <https://doi.org/10.1021/acscatal.6b02552>.
6. Arshad, F.; ul Haq, T.; Khan, A.; Haik, Y.; Hussain, I.; Sher, F. Multifunctional Porous NiCo Bimetallic Foams toward Water Splitting and Methanol Oxidation-Assisted Hydrogen Production. *Energy Convers. Manag.* **2022**, *254*, 115262. <https://doi.org/10.1016/j.enconman.2022.115262>.
7. Zhao, B.; Xu, C.; Shakouri, M.; Feng, R.; Zhang, Y.; Liu, J.; Wang, L.; Zhang, J.; Luo, J.-L.; Fu, X.-Z. Anode-Cathode Interchangeable Strategy for in Situ Reviving Electrocatalysts’ Critical Active Sites for Highly Stable Methanol Upgrading and Hydrogen Evolution Reactions. *Appl. Catal. B Environ.* **2022**, *305*, 121082. <https://doi.org/10.1016/j.apcatb.2022.121082>.
8. Li, J.; Xing, C.; Zhang, Y.; Zhang, T.; Spadaro, M.C.; Wu, Q.; Yi, Y.; He, S.; Llorca, J.; Arbiol, J.; et al. Nickel Iron Diselenide for Highly Efficient and Selective Electrocatalytic Conversion of Methanol to Formate. *Small* **2021**, *17*, 2006623. <https://doi.org/10.1002/smll.202006623>.
9. Li, J. Nickel-Organic Frameworks as Highly Efficient Catalyst for Electrochemical Conversion of CH₃OH into Formic Acid. *Electrochim. commun.* **2023**, *146*, 107416. <https://doi.org/10.1016/j.elecom.2022.107416>.
10. Si, F.; Liu, J.; Zhang, Y.; Zhao, B.; Liang, Y.; Wu, X.; Kang, X.; Yang, X.; Zhang, J.; Fu, X.Z.; et al. Surface Spin Enhanced High Stable NiCo₂S₄ for Energy-Saving Production of H₂ from Water/Methanol Coelectrolysis at High Current Density. *Small* **2023**, *19*, 2205257. <https://doi.org/10.1002/smll.202205257>.
11. Abdullah, M.I.; Hameed, A.; Zhang, N.; Islam, M.H.; Ma, M.; Pollet, B.G. Ultrasonically Surface-Activated Nickel Foam as a Highly Efficient Monolith Electrode for the Catalytic Oxidation of Methanol to Formate. *ACS Appl. Mater. Interfaces* **2021**, *13*, 30603–30613. <https://doi.org/10.1021/acsami.1c06258>.
12. Ma, Y.; Li, L.; Zhang, Y.; Jian, N.; Pan, H.; Deng, J.; Li, J. Nickel Foam Supported Mn-Doped NiFe-LDH Nanosheet Arrays as Efficient Bifunctional Electrocatalysts for Methanol Oxidation and Hydrogen Evolution. *J. Colloid Interface Sci.* **2024**, *663*, 971–980. <https://doi.org/10.1016/j.jcis.2024.02.191>.